Global and Planetary Change 223 (2023) 104077

Contents lists available at ScienceDirect

Global and Planetary Change

journal homepage: www.elsevier.com/locate/gloplacha

Aquatic ecosystem response to climate, fire, and the demise of montane rainforest, Tasmania, Australia

Kristen K. Beck [a,*], Michael-Shawn Fletcher [b], Brent B. Wolfe [c], Krystyna M. Saunders [d,e]

[a] Catchments and Coasts Research Group, Department of Geography, University of Lincoln, Brayford Pool Campus, Lincoln LN6 7TS, United Kingdom
[b] School of Geography, University of Melbourne, 221 Bouverie Street, Parkville 3010, Victoria, Australia
[c] Department of Geography and Environmental Studies, Wilfrid Laurier University, 75 University Avenue West, Waterloo N2L 3C5, Ontario, Canada
[d] Australian Nuclear Science and Technology Organisation, New Illawarra Road, Lucas Heights 2234, New South Wales, Australia
[e] Institute for Marine and Antarctic Studies, University of Tasmania, 20 Castray Esplanade, Battery Point, 7004, Australia

ARTICLE INFO

Editor: Jed O Kaplan

Keywords:
Aquatic ecosystems
Fire
Climate change
Holocene
Montane rainforest
Palaeoecology
Tasmania
Australia

ABSTRACT

The 2019/2020 southeast Australian fires ravaged the environment and threatened endemic vegetation groups, including the Tasmanian montane rainforest. This endemic biome, dominated by *Athrotaxis* species and *Nothofagus gunnii,* is declining due to increased aridity and fire frequency (years between fire events). Little is known about the impacts of fire and the montane rainforest decline on aquatic ecosystems in the region, yet aquatic ecosystems are strongly reliant on the terrestrial environment for nutrients and humic acids to support their ecosystem health. Here we evaluate the impacts of repeat fires and decline in montane rainforest species on the aquatic ecosystem of Lake Osborne, Tasmania, Australia, during the past 6500 years using a palaeoecological approach. Newly obtained data including organic carbon ($\delta^{13}C$) and nitrogen ($\delta^{15}N$) isotope composition, visible reflectance spectroscopy ($R_{650–700}$ as a measure of chlorophyll *a* and derivatives), and diatom remains are compared with previously published charcoal, pollen, micro-X-Ray fluorescence, magnetic susceptibility, and organic carbon and nitrogen elemental data. Results suggest repeat fire occurrence from 6300 to 4200 years ago caused a decline in montane rainforest, increased erosion, and high aquatic productivity, pH, and conductivity (as indicated by diatoms *Epithemia* species, *Fragilaria* type species, *Karayevia clevei*, and *Tabellaria flocculosa*). Recovery of montane rainforest due to low fire activity from 4200 to 3000 years ago caused an anomalous assemblage of diatoms dominated by *Aulacoseira* species along with a less productive aquatic environment (inferred from low $\delta^{13}C$ and $\delta^{15}N$, $R_{650–700}$, and percent macrophytes and algal remains), higher lake level and clearer waters at Lake Osborne. A fire event 2500 years ago caused the removal of montane rainforest and a shift to *Eucalyptus* dominance within the catchment, leading to an increase in aquatic productivity, and a shift toward benthic diatom taxa dominant in clearer waters-characteristic of eastern Tasmanian sites. The aquatic environment at Lake Osborne for the past 6500 years has responded to increased fire frequency, declines in the montane rainforest and climate change. Fire disturbance removes montane rainforest, burns the underlying soils resulting in erosion of terrigenous material and increases aquatic productivity with communities that favour higher conductivity and low light conditions. With projected increases in fire frequency and loss of rainforest, freshwater ecosystems are vulnerable to changes in physical characteristics, productivity, species assemblages, and ecological resilience.

1. Introduction

Large catastrophic fires are an increasing threat to the natural environment that have devastating effects across the globe (IPCC, 2022). In 2019/2020, catastrophic fires ravaged an enormous area of the Australian landscape, burning approximately 1.8 million hectares in southeast Australia, threatening endemic vegetation types such as fire sensitive rainforest (Collins et al., 2021; Gallagher et al., 2021; Godfree et al., 2021). While there has been a concerted effort to understand the impacts of fire on terrestrial systems, their impacts on nearby and connected freshwater ecosystems are not well understood. Indeed, there is an overall dearth of information on the role of fire in driving persistent

* Corresponding author.
E-mail address: kbeck@lincoln.ac.uk (K.K. Beck).

https://doi.org/10.1016/j.gloplacha.2023.104077
Received 18 August 2022; Received in revised form 19 January 2023; Accepted 21 February 2023
Available online 25 February 2023

aquatic ecosystem changes. Given the precarious state of freshwater resources under pressure from human populations, land use and climatic change, and the clear dependency of freshwater quality for healthy aquatic ecosystem functioning, knowledge of the role of fire is required for the sustainable provision of freshwater resources in the future. Here we assess the long-term impacts of changing fire regimes and fire-driven landscape change on associated freshwater systems using the fire sensitive rainforests of Tasmania as a test-case.

Tasmanian rainforest, particularly higher altitude (montane) rainforests, have suffered fire-driven range contractions during recent centuries (Holz et al., 2015; Mariani et al., 2019). These montane rainforests are dominated by fire-sensitive conifers and angiosperms that are now restricted to topographic fire refugia in the mountainous landscape of this maritime continental island (Bowman et al., 2019; Cadd et al., 2019). Important conifer taxa to this system include two members of the Cupressaceae, *Athrotaxis cupressoides* D.Don and *Athrotaxis selaginoides* (Hook.) Oerst. The principal angiosperm in this system is *Nothofagus gunnii* (Hook.f.) Oerst. (Nothofagaceae), synonym *Fuscospora gunnii, N. gunnii* used here for consistency with the fossil record (sensu Hill et al., 2015). Each of these species have slow population growth, due to very long-life spans and poor dispersal, rendering them susceptible to inheriting an extinction debt (sensu Talluto et al., 2017). Changes in climate have caused reductions in their resilience to disturbance, particularly from fire (Fletcher et al., 2014; Mariani et al., 2019; Fletcher

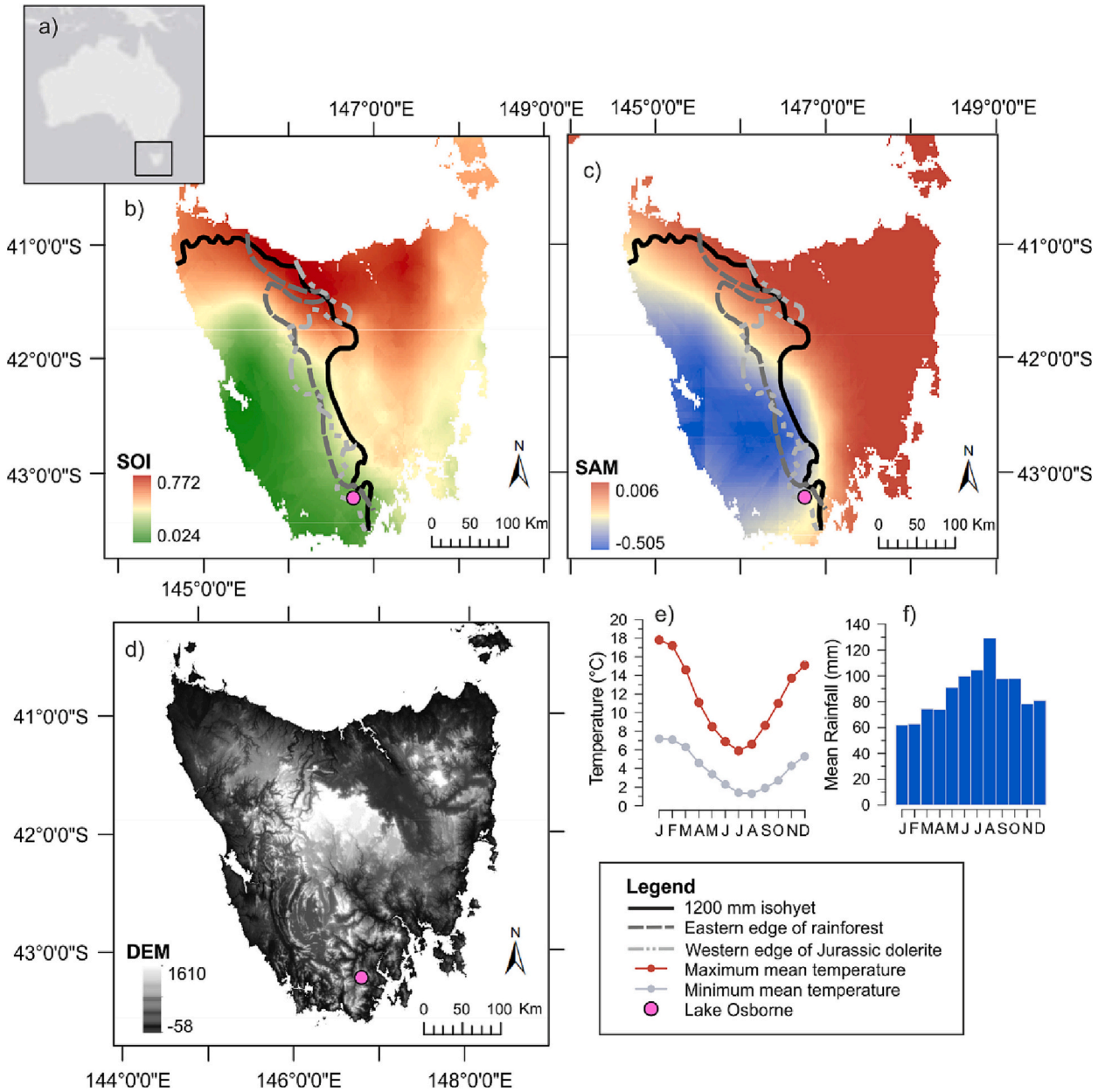

Fig. 1. a) Inset map showing location of Tasmania, Australia. b-d) Maps of Tasmania with the location of Lake Osborne (pink dot), and b & c) the extent of Tyler's line indicated by the 1200 mm isohyet limit of precipitation (black line), eastern boundary of the rainforest vegetation (grey dashed line) and western boundary of the dolerite geology (light grey dashed line) (Tyler, 1992; Rees and Cwynar, 2010). b) Map of the Southern Oscillation index, an indicator of ENSO, correlated with annual rainfall where lower values indicate more El Niño like conditions and higher values more La Niña and c) the Southern Annular Mode index correlated with annual rainfall (Mariani and Fletcher, 2017). d) Digital elevation map of Tasmania (metres above sea level) with low elevations in dark tones and high elevations in light tones. e) Mean monthly maximum (red) and minimum (grey) temperatures, and f) mean monthly rainfall (mm) for Hartz Mountain meteorological station, Keoghs Pimple, Tasmania. Climate data provided by Bureau of Meteorology (2022). (For interpretation of the references to colour in this figure legend, the reader is referred to the web version of this article.)

et al., 2020). Following fire, their seedlings and saplings show lower success and high adult mortality resulting in poor post-fire recovery (Bowman et al., 2019; Bliss et al., 2021). In contrast to the detailed understanding of how fire impacts these montane rainforests, comparatively little is known about the impact of montane rainforest loss on connected aquatic ecosystems.

Aquatic ecosystems within rainforested areas of Tasmania are almost completely dependent on the terrestrial environment for allochthonous carbon, humic acids, and nutrients from decomposing vegetation (Brown et al., 1982; Steane and Tyler, 1982; Tyler, 1992). This reliance on terrestrial ecosystems is extreme in Tasmanian systems due to the inert nature of the bedrock that underlies much of the high rainfall rainforest zone. Analyses of the long-term dynamics between terrestrial and aquatic ecosystems in this region consistently show a tight coupling between climate and disturbance-driven changes in the terrestrial environment and aquatic ecosystem dynamics within rainforest catchments (Beck et al., 2018b; Mariani et al., 2018; Beck et al., 2019). A key finding of this work is that fire-driven removal of rainforest from catchments can radically alter aquatic ecosystem dynamics and functioning (Beck et al., 2018a). Changes in the aquatic ecosystem stem principally from changes in the type of vegetation-soil system that replaces rainforest following fire. When fire-promoting plants with sclerophyllous foliage replace rainforest, there is a reduction in the organic content of soils and a reduction in the available nutrients (Bowman and Wood, 2009) and thus, the relationship aquatic ecosystems have with the terrestrial environment is altered (Beck et al., 2019).

Here, we aim to understand how the aquatic ecosystem of a lake within montane rainforest responded to both repeated high impact fires and the fire-driven removal of rainforest from within its catchment during the past 6500 years. Our study site is Lake Osborne, Tasmania, a site formally surrounded by *Athrotaxis* spp.-*N. gunnii* montane rainforest, but today is situated within a catchment dominated by fire-promoted *Eucalyptus* forest (Fletcher et al., 2018; Mariani et al., 2019; Fletcher et al., 2020). Lake Osborne is located within the Hartz Ranges at the southern tip of the Southern Ranges (Fig. 1). Lake Osborne has been the focus of several palaeoecological studies investigating relationships among fire, vegetation and landscape processes spanning the past 14,000 years (Fletcher et al., 2014; Fletcher et al., 2018; Cadd et al., 2019; Fletcher et al., 2020). *Athrotaxis* spp.-*N. gunnii* montane rainforest dominated the Hartz Range between ca. 12.0 to 8.0 ka (12,000–8000 years ago) in a mild and wet climate, free from significant fire disturbance. An increase in the frequency and severity of landscape-scale fires (i.e. fires occurring across multiple catchments (Mariani et al., 2019)) drove successive losses in *N. gunnii* (ca. 6.0 ka) and *Athrotaxis* spp. (ca. 3.0 ka) from the Lake Osborne catchment in response to an increasingly variable and drier climate, with a complete loss of rainforest and establishment of the modern Eucalypt forest occurring after ca. 3.0 ka (Fletcher et al., 2018). These fires within the catchment of Lake Osborne also had a profound impact on the soil system, with a marked reduction in soil carbon and a decrease in overall soil cover resulting in a rise in the delivery of bedrock weathering products (i.e., rare earth elements) into the lake. This temporal sequence at Lake Osborne occurs across much of the humid rainforest zone of Tasmania (Hopf et al., 2000; Stahle et al., 2016; Beck et al., 2017; Stahle et al., 2017; Mariani et al., 2018; Cadd et al., 2019; Mariani et al., 2019; Fletcher et al., 2020; Fletcher et al., 2021) and is one that has increased the overall flammability of the region's vegetation, increasing the likelihood of subsequent fire-driven rainforest loss (Fletcher et al., 2021), particularly as climate changes and human populations increase the occurrence of ignition in this landscape. The increasing dominance of *Eucalyptus* in Tasmania is not only creating vulnerability in rainforest vegetation due to its rapid growth, high flammability, and ability to prosper on low nutrient soils (Wood and Bowman, 2012; Fletcher et al., 2020; Fletcher et al., 2021), but this shift in vegetation also alters aquatic ecosystems. These vegetation shifts can cause changes in trophic status, declines in resilience and decoupling from the terrestrial environments (Beck et al., 2018a; Beck et al., 2018b; Mariani et al., 2018; Beck et al., 2019).

To meet the research aim, we employ a multiproxy palaeoecological approach of lake sediments from Lake Osborne (surface sediment cores TAS1110 SC1 and SC2), spanning ca. 6.5 ka using newly collected data of organic carbon and nitrogen isotope composition (indicators of organic matter sources), visible reflectance spectroscopy (an indicator of sediment composition), and diatom remains (indicators of aquatic ecosystem dynamics). These were compared to data published in Fletcher et al. (2014) that includes pollen (an indicator of vegetation), charcoal (an indicator of fire), organic elemental carbon and nitrogen content (indicator for organic matter source from C/N ratios), micro-X-ray Fluorescence (XRF) core scanning (an indicator of soil and other catchment processes), and magnetic susceptibility (an indicator of soil erosion). We hypothesise (1) the declines in montane rainforest species caused by fire will drive changes in the aquatic environment related to catchment processes; (2) recovery of montane rainforest will elicit the opposite response in the aquatic ecosystem compared to declining montane rainforest; and (3) the loss of the montane rainforest and shift to more sclerophyll-dominated vegetation will drive the aquatic ecosystem toward a new species composition.

1.1. Regional setting

Tasmania is a temperate island off the south-east coast of mainland Australia (Fig. 1). The island is bisected by northwest-southeast trending mountains that intercept the predominantly west to east (zonal) airflow that dominates the mid- to high-latitudes of the Southern Hemisphere. The orographic effect on wind and rainfall patterns imparted by this geography has created distinct biogeographic provinces in Tasmania. The west is characterised by a maritime climate with cool temperatures and high rainfall, organic-rich soils, and a dominance by rainforest vegetation in the absence of disturbance. The east is comparatively drier, with higher temperature fluctuations, minerogenic soils and a dominance by temperate broadleaf (*Eucalyptus*) forests and grasslands. In terms of aquatic ecosystems, the organic soils that dominate in the west have given rise to acidic dystrophic lakes with low light penetration (~2 m), while in the east, enriched mineral soils produce more alkaline lakes with higher light penetration (~10 m) (Tyler, 1992; Rees and Cwynar, 2010). These limnological characteristics create a division in aquatic species composition between east and west with a transitional corridor along the central ranges known as 'Tyler's line' (Vyverman et al., 1996; Rees and Cwynar, 2010; John, 2018). Modern interannual rainfall patterns in Tasmania are also spatially explicit, with a strong negative correlation between rainfall and the Southern Annular Mode (SAM) in western regions, while the El Niño-Southern Oscillation (ENSO) dominates in the north and east (Hill et al., 2009; Harris and Lucas, 2019). A negative SAM phase causes wet conditions in western Tasmania (Mariani and Fletcher, 2016). During El Niño, Australia experiences drier conditions and wetter conditions during La Niña (McPhaden et al., 2006), particularly in the north in Tasmania (Mariani and Fletcher, 2017). Previous studies have shown negative SAM is more dominant during stronger El Niño years, and positive SAM is more dominant during La Niña years (Gong et al., 2010; Kim et al., 2017). Since Lake Osborne is located on the edge of the influence of both SAM and ENSO, during positive SAM and El Niño years, dry conditions are exacerbated. Since the late Holocene, ENSO has increased in strength and variability, with a high frequency of strong El Niño events (Donders et al., 2008; Beck et al., 2017).

Lake Osborne is a small (0.02 km^2) glacially formed lake that was established around 14.0 ka (Fig. 1). The lake is acidic and ultra-oligotrophic, 10 m deep and subalpine, located at 920 masl within a small catchment (Knott et al., 1978; Ling et al., 1989; Fletcher et al., 2014; Mariani et al., 2019). Soils are acidic and poorly drained with geology consisting of a mixture of dolerite and periglacial deposits, and an unyielding bedrock with relatively high nutrient potential (Knott et al., 1978; Fletcher et al., 2014; Fletcher et al., 2018). The mean

maximum annual temperature is 11.4 °C and mean annual rainfall is 1087.0 mm determined by the nearest meteorological station at Hartz Mountain, Keoghs Pimple, 1.8 km from Lake Osborne (43.20°S, 146.77°E, 831 masl) (Bureau of Meteorology, 2022). The local vegetation is a mixture of low-lying sedge vegetation *Gahnia grandis*, and Proteaceous shrubs (*Bellendena montana, Orites revolutus, Hakea lissosperma and Telopea truncate*), as well as forest taxa *Eucalyptus coccifera*, *Nothofagus cunninghamii,* and *Eucryphia milliganii,* with a few fire scarred *Athrotaxis selaginoides* (Cupressaceae) on the shoreline (Fletcher et al., 2014; Fletcher et al., 2018; Mariani et al., 2019). Lake Osborne is located on the southern end of Tyler's line near the transition between the SAM and ENSO rainfall correlation zones (Fig. 1).

2. Materials and methods

2.1. Core collection and analyses

In 2011, two surface sediment cores (TAS1110SC1 and TAS1110SC2, 85 cm and 91 cm in length, respectively) spanning ca. 6.5 ka were collected using a Universal Corer (Aquatic Research Instruments, 2018) from the deepest point (10 m) of Lake Osborne (Fletcher et al., 2014). In this study we used previously published data from Fletcher et al. (2014) including radiometric dating, charcoal, pollen, XRF, magnetic susceptibility, and organic carbon and nitrogen content, with newly collected data of organic carbon and nitrogen isotope composition, visible reflectance spectroscopy, and diatom remains from TAS1110SC2. XRF was performed on TAS1110SC1, and radiometric dating, pollen, charcoal, diatoms, and visible reflectance spectroscopy was performed on TAS1110SC2. The magnetic susceptibility was performed on both cores to align them (see Fletcher et al., 2014).

2.2. Chronology

The chronology was revised from Fletcher et al. (2014) with the latest SHcal20 calibration curve (Hogg et al., 2020). The sediment core chronology was derived from three ^{210}Pb dates, out of a total of five analysed samples using gamma spectroscopy at the University of Pittsburgh (Pittsburgh, USA), as the top three had sufficient unsupported ^{210}Pb material to be used by the *plum* age-depth modelling package (Aquino-López et al., 2018). Eight bulk sediment radiocarbon dates (Fig. 2) were analysed by the NoSAMS radiocarbon laboratory (Woods Hole, Massachusetts, USA) and included in the *plum* age-depth model. The same five samples were analysed for ^{137}Cs, but only one sample detected levels of ^{137}Cs and therefore was excluded from the age-depth model due to low sample resolution. The radiometric dating results included in the age-depth model are presented in the Supplementary data (Table S1 and S2) and Fletcher et al. (2014). The revised age-depth model was performed using the *plum v.0.2.2* package in *R v.4.0.4* (R Core Team, 2021). *Plum* utilises Bayesian statistical modelling to accurately determine age-depths from raw (supported and unsupported) ^{210}Pb concentrations and can produce ages beyond standard Constant Rate of Supply models (Aquino-López, 2018). The age-depth modelling in *plum* uses the *bacon* Bayesian statistical non-gaussian autoregressive approach to determine sediment accumulation rates with prior distributions using self-adjusting Markov chain Monte Carlo iterations (Blaauw and Christen, 2011). Accumulation rates calculated using the updated age-depth model does not considerably differ from the previously published data by Fletcher et al. (2014), apart from in the top 10 cm, which spans the past ~970 years (see comparison of accumulation rates in Supplementary data (Fig. S1)).

2.3. Pollen and charcoal analysis

Pollen and charcoal data were retrieved from Fletcher et al. (2014). Pollen analysis was performed every 0.5 cm for the top 10 cm, except from 7.5 to 9.5 cm and the remainder of the core, which was performed at 1 cm resolution (average 61 year resolution) using standard methods (Faegri and Iversen, 1989). A minimum of 300 terrestrial pollen grains were identified, and the relative abundance was determined using the total of terrestrial pollen grains. Relative abundance of the terrestrial pollen was determined using the sum of terrestrial grains, and aquatic pollen and spore relative abundance was calculated using the sum of terrestrial grains, aquatic pollen, and spores. In this study, a Principal Components Analysis (PCA) was performed to determine the dominant

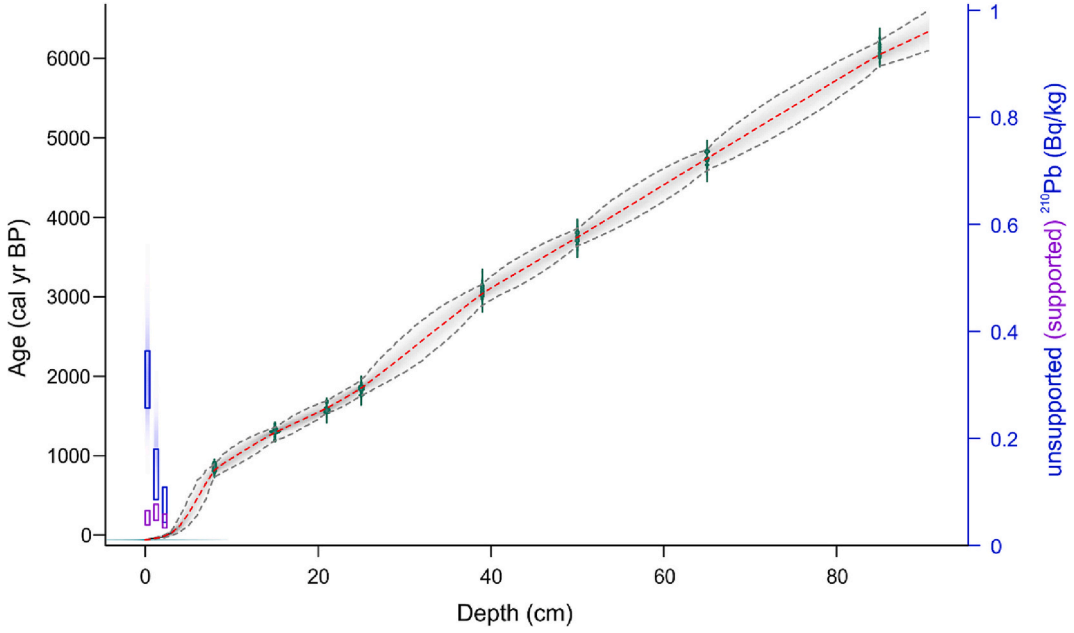

Fig. 2. Updated age-depth model for Lake Osborne using the latest calibration curve (SHCal20) and *plum* age-modelling package in *R*. Blue rectangles indicate the activity of unsupported ^{210}Pb and the purple rectangles indicate the supported ^{210}Pb. The green symbols are the calibrated radiocarbon measurements. The red dashed line is the determined age-depth model chosen by the weighted means and the grey dashed lines show the 95% confidence intervals of the model. (For interpretation of the references to colour in this figure legend, the reader is referred to the web version of this article.)

trends across the multivariate pollen data to compare to other proxy data. A PCA was performed on the percentage terrestrial pollen taxa from −20 to 6300 calendar years Before Present (cal yr BP) using the rda function in the *vegan v. 2.5–7* package (Oksanen et al., 2019) in *R v.4.0.4* using the standardization method (i.e. scaled around a mean of zero with a unit of variance). The top four data points were removed to combat arch effects in the PCA (see Supplementary data Fig. S2 for more PCA biplot output).

Accumulation rates of microscopic (MicroChar) and macroscopic (MacroChar) charcoal were recalculated for this study using the raw counts obtained from Fletcher et al. (2014) due to the revised age-depth model. MicroChar was identified alongside pollen grains and concentration was determined using the exotic pollen spike (*Lycopodium* spp.) and sediment accumulation rates. MacroChar was processed at a resolution of 0.5 cm (36-year resolution on average) by digesting 1–1.5 cm^3 of sediment in 30% hydrogen peroxide until all reactions were complete. To identify macroscopic charcoal, material was sieved and identified by two fractions (>250 μm and 250–125 μm). For more information on the methods used see Fletcher et al. (2014). In Fletcher et al. (2014), MacroChar accumulation rates and significant peaks were determined by CHARAnalysis (Higuera, 2009). Since Fletcher et al. (2014), CHARAnalysis has been replaced by the *R* package *tapas* (Finsinger and Bonnici, 2022). Thus, here MacroChar accumulation was determined from the combined two fractions and the updated age-depth model using the *tapas v.0.1.0*. The trends in accumulate rate of the MacroChar show little to no difference between the CHARAnalysis outputs (Fletcher et al., 2014) and the *tapas* outputs presented here (see Supplementary data Fig. S3). Additionally, the significant peaks showed very similar outputs with an additional recent peak (−26 cal yr BP) from the CHARAnalysis MacroChar model output and an additional older peak (6210 cal yr BP) in the *tapas* MacroChar model output (present study). However, to avoid any methodological discrepancies between the models, the significant peaks identified in Fletcher et al. (2014) were used in this study and mapped onto the MacroChar in Fig. 3. See Supplementary data Fig. S3 for more details on CHARAnalysis and *tapas* model outputs.

2.4. Diatoms and visible reflectance spectroscopy

Diatoms were processed at 2 cm resolution (with exception of depths 8.5, 10.5, and 12.5 cm due to low amounts of material), equivalent to, on average 145-year resolution. A sample volume of 0.5 mL of sediment was digested using the hydrogen peroxide method from Battarbee (1986) and mounted using Naphrax®. A minimum of 300 valves were counted at 1000× magnification using an oil immersion DIC objective. Diatom concentration was determined by known volumes of sediment evaporated onto a cover slip (Battarbee, 1986). Taxonomic names of identified species were verified using Algaebase (https://www.algaebase.org/) (see Supporting data Table S3). Species are represented as relative abundances of all identified taxa per sample depth. The total *Gomphonema* and *Epithemia* species were combined due to high abundances of undecipherable valves in girdle view. PCA was used to determine the dominant trends across the multivariate diatom species data to compare to other proxy data from the Lake Osborne record. A PCA was performed on the diatom percentage data with a maximum abundance of at least 3% and at least two occurrences using the rda function in the *vegan v.2.5–7* package (Oksanen et al., 2019) in *R* with the normalization method (i.e. creating a sum of squares margin equal to one) (see Supplementary data Fig. S4 for more PCA biplot output).

Reflectance spectroscopy in the visible light range (380–730 nm) is a non-destructive scanning technique used to describe sediment composition (Rein and Sirocko, 2002; Wolfe et al., 2006). The area of the reflectance trough in the red spectrum between 650 and 700 nm ($R_{650–700}$) is useful for estimating the total amount of chlorophyll *a* and derivatives, while the ratio between 660 and 670 nm ($R_{660/670}$) may be used as an indicator of pigment diagenesis (Wolfe et al., 2006; Saunders et al., 2012; Saunders et al., 2013; Van Exem et al., 2018). Scanning visible reflectance spectroscopy was performed at 0.2 cm resolution (14-year resolution on average) using a Gretag-Spectrolino (GretagMcBeth, Switzerland) at the University of Bern, Switzerland.

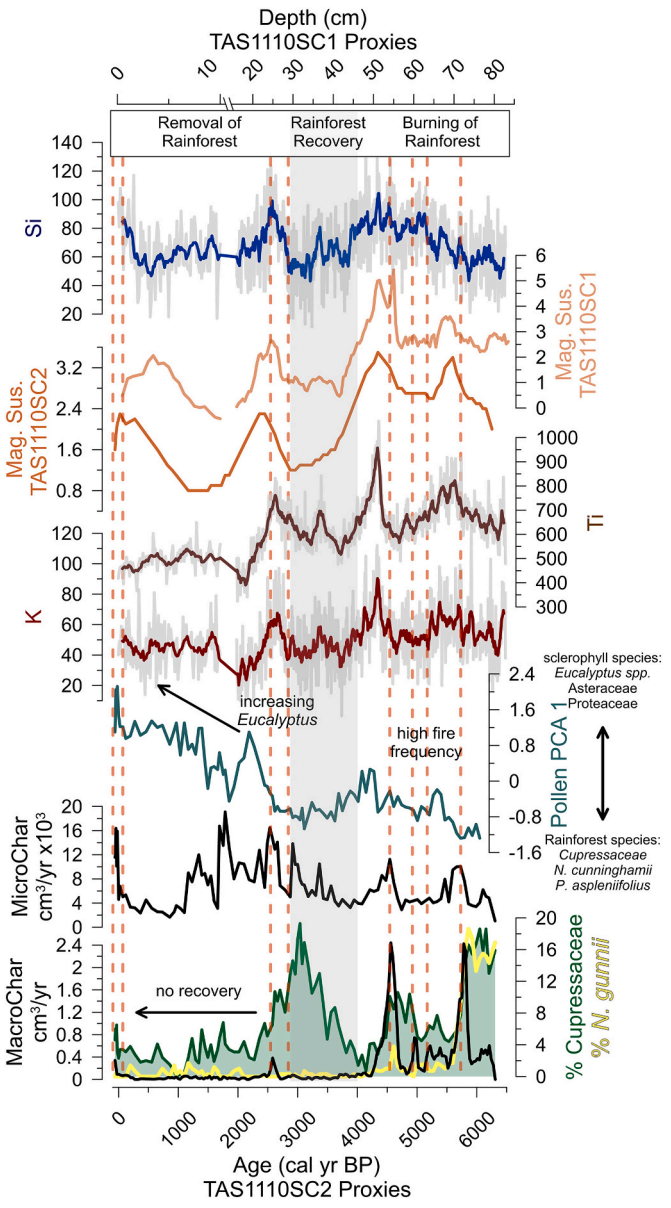

Fig. 3. Terrestrial proxy summary for Lake Osborne. Top to bottom: XRF silica (Si) (blue) fitted with a weighted average (window = 9), magnetic susceptibility for TAS1110SC1 (light orange), magnetic susceptibility for TAS1110SC2 (orange), XRF titanium (Ti) (brown) fitted with a weighted average (window = 9), XRF potassium (K) (red) fitted with a weighted average (window = 9), pollen PCA axis 1 (teal) with an explained variance of 13.5%, where high values indicate more sclerophyll species and low values more rainforest taxa, microscopic charcoal (MicroChar) accumulation rate (cm^3/yr x 10^3) (black), percent Cupressaceae (green) and *Nothofagus gunnii* (yellow) pollen, and macroscopic charcoal (MacroChar) accumulation rate (cm^3/yr) (black). Red vertical dashed lines indicate the significant MacroChar peaks determined by Fletcher et al. (2014), and the grey shaded area highlights the montane rainforest recovery period. XRF indicators and magnetic susceptibility are performed on TAS1110SC1 and plotted by depth (cm), all other proxies were performed by TAS1110SC2 and plotted by age (cal yr BP). (For interpretation of the references to colour in this figure legend, the reader is referred to the web version of this article.)

2.5. Geochemical measurements

Organic carbon and nitrogen content results were originally published in Fletcher et al. (2014); however, the carbon and nitrogen isotope data are new to this study. Subsamples of wet sediment at 0.5 cm resolution (35-year resolution on average) were treated with 10% HCl at 60 °C for 2 h to remove carbonates and then rinsed with deionized water until neutral. Samples were then freeze-dried and sieved with a 500 μm mesh to remove coarse materials. Samples were analysed for elemental and isotopic composition of organic carbon and nitrogen using a continuous flow isotope ratio mass spectrometer (CF-IRMS) at the University of Waterloo Environmental Isotope Laboratory, Canada. The Carbon/Nitrogen ratio (C/N) was determined by percent weights of carbon and nitrogen. Organic carbon and nitrogen isotope ratios are reported as $\delta^{13}C$ (‰) relative to the Vienna-Peedee Belemnite (VPDB) standard, and $\delta^{15}N$ (‰) relative to atmospheric nitrogen (AIR), respectively. Analytical uncertainty was ±0.2‰ and ± 0.3‰ for $\delta^{13}C$ and $\delta^{15}N$, respectively.

XRF and magnetic susceptibility data were retrieved from Fletcher et al. (2014) at a resolution of 0.1 cm and 1 cm (7-year and 71-year average resolution), respectively. Only a subset of XRF data are used in this study. K and Si are used as indicators of soil constituents and Ti is used as an indicator for erosion of terrigenous material (Croudace and Rothwell, 2015). Mn/Fe ratios are indicative of redox conditions, where higher Mn/Fe suggests anoxic conditions and greater redox potential (Marsh et al., 2007; Croudace and Rothwell, 2015).

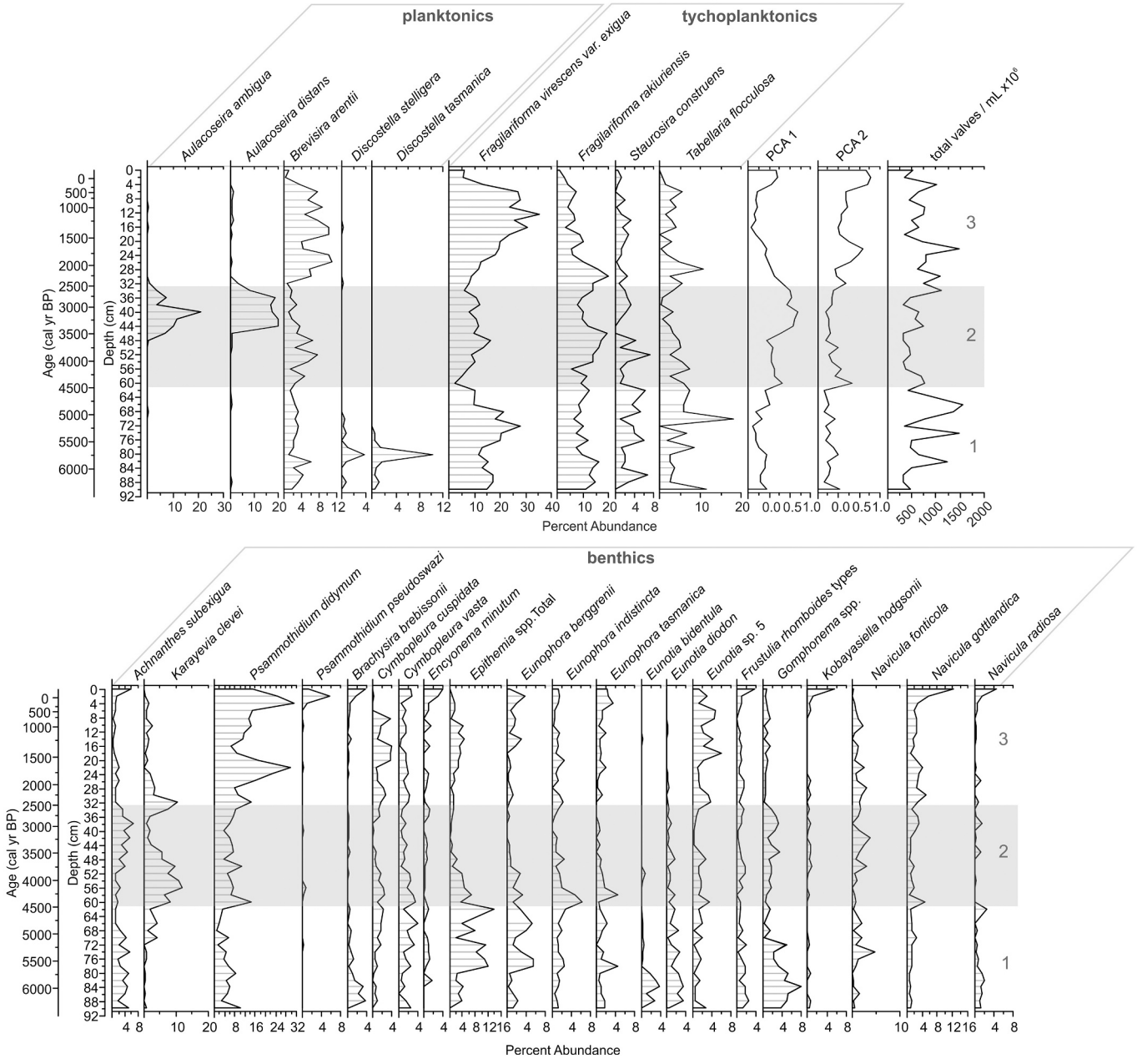

Fig. 4. Stratigraphic plots of the most abundant diatom species (>3% abundance in at least two samples) presented as percent relative abundance. Diatom species are grouped by planktonic and tychoplanktonic (upper panel), and benthic taxa (lower panel). PCA axes 1 and 2 estimate trends in the multivariate diatom percentage data. Key intervals separated by grey box, determined by transitions across all proxies, 1) burning rainforest, 2) rainforest recovery, and 3) loss of rainforest. The orange dashed line indicates the ca. 4.5 ka fire event.

3. Results and discussion

3.1. Summary of Lake Osborne multi-proxy record

Results from the multi-proxy record from Lake Osborne spanning ca. 6.5 ka demonstrate three key intervals of terrestrial environmental change related to fire and vegetation change: (1) burning rainforest, (2) rainforest recovery, and (3) loss of rainforest (Fig. 3). The aquatic ecosystem responded to the changing terrestrial environments of these intervals with higher productivity during intervals of low rainforest and shifts in conductivity and pH with changing fire activity (Figs. 4 and 5).

3.2. Aquatic ecosystem response to burning montane rainforest

During the high fire frequency period (on average 384 cal yr BP between significant fire events) from ca. 6.5 to 4.2 ka, the aquatic ecosystem was a productive alkaline and conductive environment due to increased erosion with burning of the montane rainforest. Declines in montane rainforest taxa (Cupressaceae *Athrotaxis* spp. and *N. gunnii*) and other rainforest taxa (*N. cunninghamii* and *Phyllocladus asplenifolius*) (Fletcher et al., 2014), captured by a positive trend in the pollen PCA axis 1 (see Fig. S1 in Supporting data for more detail on the PCA results), occurred with peaks in MacroChar and MicroChar (Fig. 3). These fire events resulted in increased erosion into Lake Osborne indicated by increased Ti and magnetic susceptibility (Fig. 3). As fires burn organic soils, they erode terrigenous material from the landscape into nearby waterbodies (di Folco and Kirkpatrick, 2011; Morris et al., 2015). During this frequent fire interval, planktonic *Discostella stelligera* and *Discostella tasmanica*, tychoplanktonic *F. virescens* var. *exigua*, *F. rakiuriensis, S. construens,* and *T. flocculosa,* and benthic *Epithemia* and *Gomphonema* spp. dominated. These diatom taxa are tolerant of higher pH and conductivity (John, 2018). Catchment erosion from fire activity would have transported terrigenous material and dissolved constituents (e.g. K and Si, Fig. 3) creating a conductive aquatic environment (Abraham et al., 2017). *Discostella* spp. only occurred in this early part of the record and indicate many possible limnological conditions including: higher conductivity (Fritz et al., 2019), nutrient availability (Saros et al., 2012; Saros et al., 2014; Malik et al., 2017), and lower light conditions (i.e. mixing depth) (Saros et al., 2014; Saros et al., 2016; Malik et al., 2017). Higher inputs of terrigenous material from the landscape provided more nutrients and base cations to the lake, which would have blocked light penetration and thus resulted in shallower mixing depths, supporting the ecological preferences of *Discostella*. Similar patterns of increased *D. stelligera* dominance related to fire and disturbance were also observed in a sediment core record from Lake Vera, Tasmania (Beck et al., 2019). Following the ca. 4.5 ka fire event, percent abundance of Cupressaceae is low and *K. clevei* increased in abundance, a species with a preference for high conductivity and alkaline conditions (John, 2018). This transition was coeval with peaks in conductivity and erosion indicators, K, Si, Ti, and magnetic susceptibility (Fig. 3). This suggests that the ca. 4.5 ka fire event had considerable impacts on the aquatic environment.

Other aquatic indicators suggest aquatic productivity was high during this interval of high fire frequency and burning of montane rainforest (Fig. 5). Increases in diatom valves and $R_{650–700}$ (i.e. chlorophyll *a* and derivatives (Wolfe et al., 2006)) at Lake Osborne suggest increased aquatic production (Fig. 5). Diatom valve concentrations peaked at ca. 5.8, 5.3 and 4.9 ka, coeval with fire activity (Fig. 5). Burning of the catchment can cause a pulse response of nutrient inputs followed by long-term declines with slow recovery of the terrestrial environment (Dunnette et al., 2014; Fletcher et al., 2014). This is apparent at Lake Osborne, where fire strips the landscape, creating a pulse of terrigenous material supporting diatom productivity, followed by rapid declines with the slow recovery of the montane rainforest (Fig. 3). Increases in macrophyte pollen, percent abundance *Botryococcus* + *Pediastrum* spp., $\delta^{13}C$, and $\delta^{15}N$ also suggest increased aquatic productivity during this

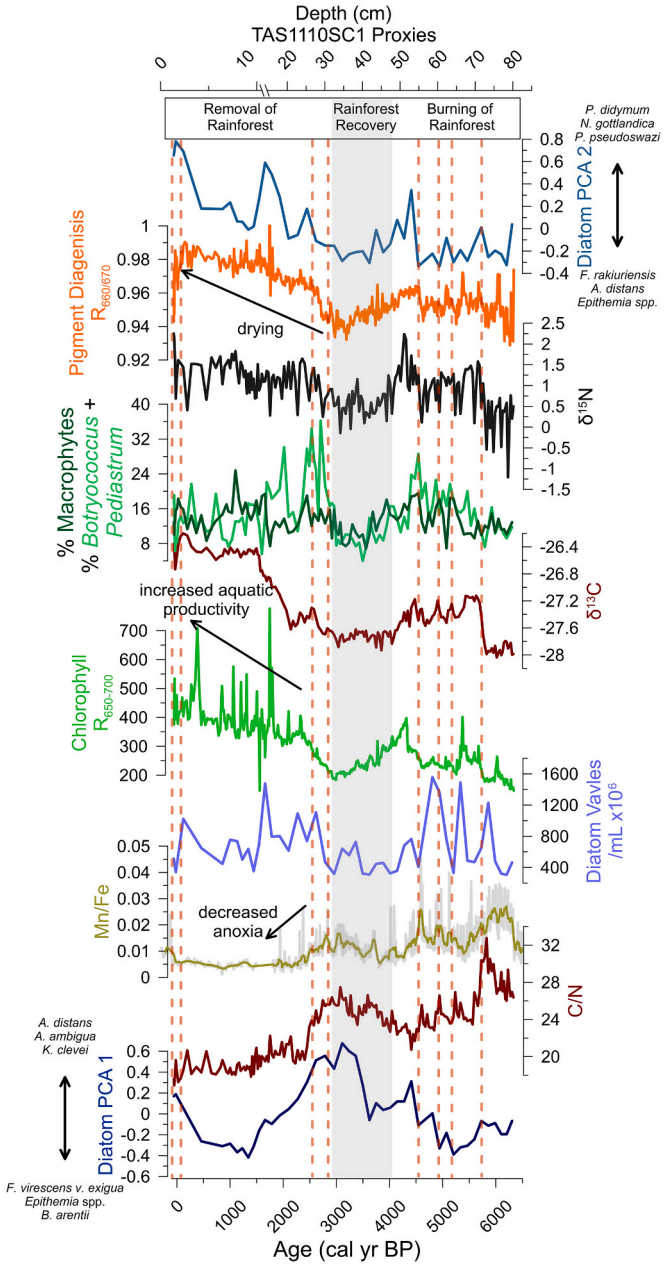

Fig. 5. Summary of Lake Osborne aquatic proxies top to bottom: diatom PCA axis 2 -high values indicate eastern Tasmanian and low values western/cosmopolitan Tasmanian species (blue), pigment diagenisis indicated by $R_{660/670}$ (orange), $\delta^{15}N$ (‰) (black), percent macrophyte pollen (dark green), percent *Botryococcus* + *Pediastrum* spp. (light green), $\delta^{13}C$ (‰) (dark red), chlorophyll indicated by $R_{650–700}$ (light green), diatom valve concentration (valves/mL x 10^6) (light blue), XRF Mn/Fe ratio (olive) fitted with a weighted average (window = 9), Carbon/Nitrogen ratio (dark red), and diatom PCA axis 1 -high values indicate more *Aulacoseira* species and low values indicate species tolerant of higher pH (dark blue). Red dashed lines indicate the significant MacroChar peaks determined by Fletcher et al. (2014), and the grey shaded area highlights the montane rainforest recovery period. XRF Mn/Fe was performed on TAS1110SC1 and plotted by depth (cm), all other proxies were performed on TAS1110SC2 and plotted by age (cal years BP). (For interpretation of the references to colour in this figure legend, the reader is referred to the web version of this article.)

interval (Fig. 5).

Fletcher et al. (2014) suggested organic carbon and nitrogen elemental indicators from Lake Osborne were terrestrially derived, which is typically the case for C/N values above ~15 (Meyers and Teranes, 2001; Lamb et al., 2006; Leng et al., 2006). However, the similarity between the $\delta^{13}C$, $\delta^{15}N$ and $R_{650–700}$ (i.e., chlorophyll *a* and derivatives), and to a lesser extent, the other aquatic productivity indicators (percent abundance macrophytes, *Botryococcus* + *Pediastrum* spp., and diatom valve concentrations; Fig. 5), suggest the organic carbon and nitrogen are aquatically derived. Nearby Duckhole Lake in southeastern Tasmania also showed high correspondence between trends in organic matter and $R_{650–700}$, with high C/N signatures (>20) (Saunders et al., 2013). At Lake Osborne, a distinct increase in $\delta^{13}C$ at ca. 5.8 ka is unlikely related to (1) changing vegetation, as rainforest vegetation has higher $\delta^{13}C$ than *Eucalyptus* species (Wood et al., 2011; di Folco and Kirkpatrick, 2013); or (2) algal inputs which tend to have lower $\delta^{13}C$ signatures (Meyers and Teranes, 2001; Leng et al., 2006). Therefore, changes in $\delta^{13}C$ and $\delta^{15}N$ are most likely related to algal productivity. Aquatic organisms will preferentially incorporate dissolved constituents containing the lighter isotope, ^{12}C and ^{14}N – classic Rayleigh Distillation (Talbot and Johannessen, 1992; Talbot, 2001). Thus, episodes of high aquatic productivity and demand on dissolved inorganic carbon and nitrogen can potentially lead to ^{13}C and ^{15}N enrichment preserved in the organic remains in lake sediments (Wolfe et al., 1999; Talbot and Lærdal, 2000; Meyers and Teranes, 2001; Wolfe et al., 2001; Leng et al., 2006). The unusually high C/N values may be the result of low availability of dissolved nitrogen. We suggest high aquatic productivity at this time is related to the removal of montane rainforest by fire, causing erosion and inputs of terrigenous material high in organic carbon that promoted algal and plant growth (Bowman and Jackson, 1981; Townsend and Douglas, 2000; di Folco and Kirkpatrick, 2013; Beck et al., 2018a).

3.3. Aquatic ecosystem response to recovery of Montane rainforest

From ca. 4.2 to 3.0 ka fire was nearly absent and Cupressaceae began to recover (Fig. 3), coeval with a shift in aquatic productivity and diatom assemblages. As Cupressaceae recovered at ca. 4.0 ka, *K. clevei* declined along with the majority benthic taxa, except for *A. subexigua* and *Gomphonema* spp., and are replaced by *Aulacoseira* spp. from ca. 3.6 to 2.4 ka (Fig. 4). Dominance of *Aulacoseira* spp. may indicate a slight increase in acidity and oligotrophy with recovery of montane rainforest; however, the planktonic nature of this genus suggests a change in lake level and/or mixing depth. *Aulacoseira* spp. are heavy siliceous planktonic taxa that prefer deeper mixing depths (Saros et al., 2016). The most dominant species of *Aulacoseira* in this record, *A. distans* and *A. ambigua*, have high light requirements (Kilham et al., 1986). Therefore, increased lake level with precipitation will favour these taxa (Brugam et al., 1998; Verschuren et al., 2000). Declines in diagenesis of pigments ($R_{660–670}$) indicate wetter conditions and/or higher lake levels as well (Fig. 5), conditions that favour greater pigment preservation (Saunders et al., 2012). The other aquatic indicators show a less productive aquatic environment during this interval with low diatom valve concentrations, percent abundance of macrophytes and *Botryococcus* + *Pediastrum* spp., $R_{650–700}$, and $\delta^{13}C$ and $\delta^{15}N$ values (Fig. 5). Low aquatic productivity accompanying montane rainforest recovery is most likely due to the absence of fire and decline in the supply of terrigenous sourced nutrients.

3.4. Aquatic ecosystem impacts from removal of montane rainforest

The loss of montane rainforest and shift toward Eucalypt forest had the greatest impact on the aquatic environment at Lake Osborne. Fire events at ca. 3.0 ka and 2.5 ka caused the final decline in montane rainforest (Cupressaceae), as well organic soil constituents (K and Si), and shift in vegetation toward increased *Eucalyptus* species (pollen PCA 1). This change in fire regime and vegetation was likely the result of the amplification of El Niño years causing drier conditions in Tasmania (Beck et al., 2017; Mariani and Fletcher, 2016; Fletcher et al., 2014). The diatom taxa present at this time (*P. didymium, N. gottlandica, B. arentii,* and *F. virescens* var. *exigua*) suggest lower pH with low conductivity (Vyverman et al., 1995; John, 2018). Increases in diatom PCA axis 2 during this interval follow the increase in *Eucalyptus* vegetation after fire events at ca. 3.0 and 2.5 ka (diatom PCA 2 vs. pollen PCA 1). Diatom PCA axis 2 is affiliated with benthic species *P. didymium, N. gottlandica, P. pseudoswazi, K. hodgsonii,* and *Eunotia* sp. 5, and loss of the anomalous *Aulacoseira* spp. These species represent a shift from a classic corridor or western assemblage to a more eastern assemblage with lower lake colour (gilvin) tolerances (Vyverman et al., 1995). This is consistent with eastern catchments, which have greater abundance of *Eucalyptus* forests and enriched mineral soils (Tyler, 1992). The high abundance of benthic taxa at this time also suggests potential lower lake levels or higher water clarity, with the exception of an increase in *B. arentii*, a planktonic taxa indicative of dystrophic western lakes (Vyverman et al., 1995, John, 2018). Eucalypt forest is found on shallow organic soils with lower nitrogen, carbon, and phosphorous content (Wood et al., 2011). Inconsistent with this low nutrient environment is increased $\delta^{13}C$ and $\delta^{15}N$, suggesting an increase in aquatic productivity consistent with increased diatom valve concentration, $R_{650–700}$ (chlorophyll *a* and derivatives), percent abundance of macrophytes and *Botryococcus* + *Pediastrum* spp. (Fig. 5). Although the material coming into the lake is likely organic poor, the amount of mineral material entering the lake may support an increase in aquatic production in an ultra-oligotrophic environment. The decrease in organic inputs under Eucalypt forests also support the increased oxic conditions of the lake (lower Mn/Fe; Fig. 5). When there is more organic matter within a freshwater environment, there is an increase in decomposition, consuming available O_2, creating anoxic conditions and mobilising Fe^{+2} and Mn^{+2} (Koinig et al., 2003; Dean and Doner, 2012). An increase in water clarity is also supported by lower Mn/Fe values. Mn/Fe are indicative of redox potential in lakes where lower Mn/Fe suggest higher concentrations of O_2 in the lake bottom (Mariani et al., 2018).

3.5. Implications of declining rainforest and increasing Eucalyptus on aquatic environments

Catchment characteristics are key to contemporary lake water quality, and in Tasmania these characteristics are dictated by vegetation and fire regimes (Fig. 6). The development of rainforest in Tasmania during the Holocene produced organic acidic peat soils rich in humic acids (Macphail, 1979; Wood and Bowman, 2012). While Tasmanian soils are considered nutrient poor, rainforests tend to have thicker peaty soils with higher total carbon, nitrogen, and phosphorous than soils under Eucalypt forests or sedgelands (Wood et al., 2011; di Folco and Kirkpatrick, 2013). These catchment characteristics such as vegetation, soil development, and geology are the defining features of the unique Tasmanian freshwater ecology and physiology. For instance, contemporary dystrophic freshwaters of Tasmania, which are defined by their tea-stained colour from high humic acid content, are not simply defined by rainforest vegetation and peaty soils, but also the Precambrian-Ordovician volcanic sediments which influence the water colour. In contrast, lakes surrounded by dolerite, such as Lake Osborne, will have clearer waters even if the catchment is heavily rainforested (Tyler, 1992). What is common among the oligotrophic to ultraoligotrophic lakes of the west, corridor and east of Tasmania, is that aquatic ecosystems are heavily reliant on the terrestrial environment for inputs of nutrients and organics (Tyler, 1992; Beck et al., 2018b; Beck et al., 2019). However, fire disrupts these terrestrial-aquatic ecosystem relationships causing an invasion of sclerophyll species such as *Eucalyptus* (Beck et al., 2018b, Beck et al., 2019) (Fig. 6). *Eucalyptus* is a pyrophytic genus that uses fire to improve its recruitment over rainforest species (Mariani et al., 2019; Fletcher et al., 2020; Fletcher et al., 2021).

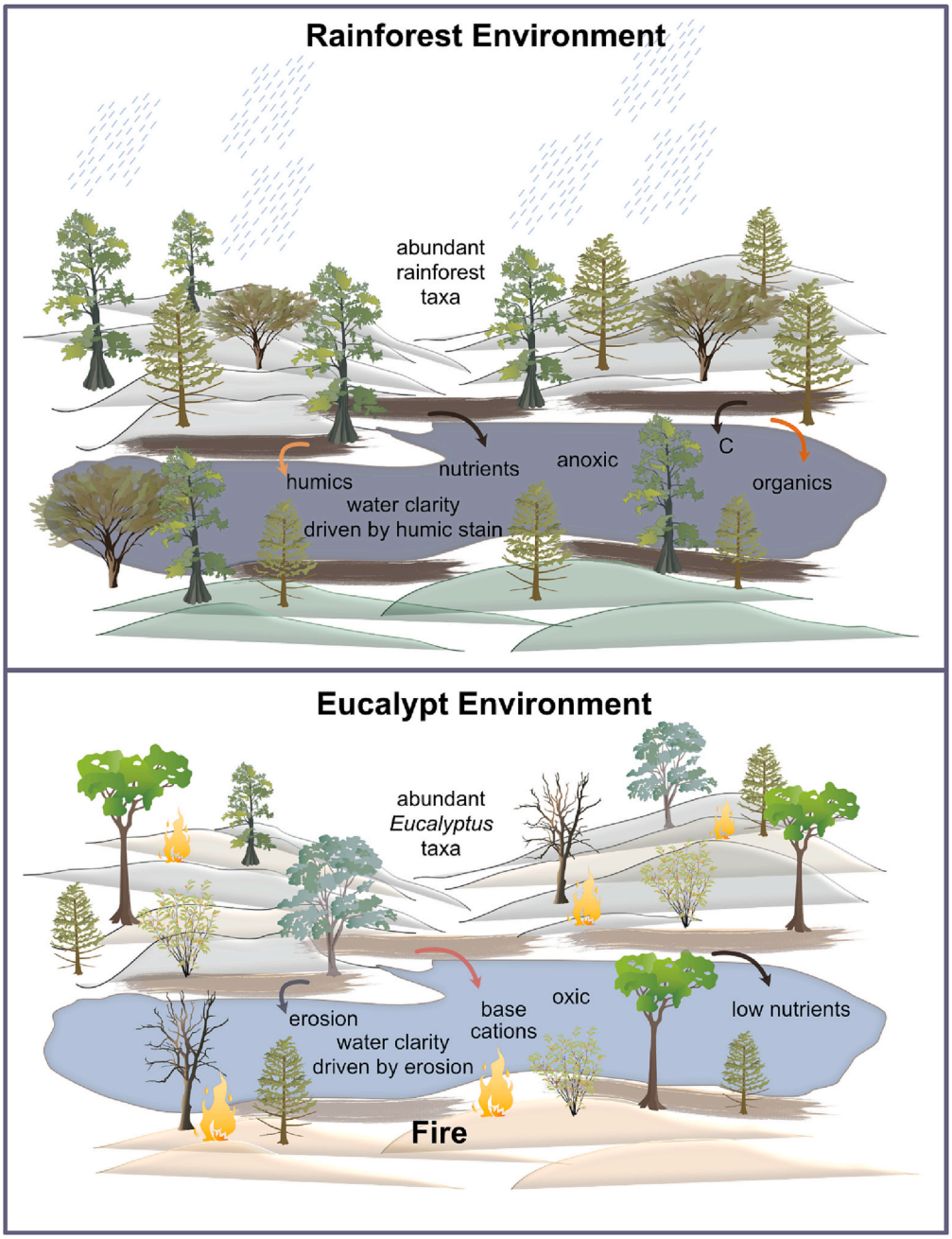

Fig. 6. Schematic representation of landscape processes occurring under a wet rainforest environment (top) and *Eucalyptus* pyrophytic environment (bottom).

Eucalyptus promote fire through high flammability of tissues, creating high fuel loads, fast recovery from fires, seed germination tolerant of fire, and heat protected bark (Brooks et al., 2004; Fletcher et al., 2020). They are also adaptive to low nutrient soils and produce nutrient-poor litter creating less favourable conditions for rainforest (Bowman et al., 1986; Orians and Milewski, 2007; Wood et al., 2011). As demonstrated by Fletcher et al. (2021), increased fire activity and dryness allows *Eucalyptus* to invade an area. With enough recruitment of *Eucalyptus*, this sclerophyll vegetation will promote further fire activity, causing a positive feedback loop for increased flammability, decreases in rainforest and further increase in *Eucalyptus* abundance (Cadd et al., 2019).

Palaeolimnological evidence indicates that changes in fire regimes and catchment dynamics related to *Eucalyptus* invasion can affect the aquatic ecosystems of Tasmania (Figs. 3, 4 and 5). At Lake Osborne, the erosive environment caused by fire activity during the dry intervals promoted aquatic production in a typically ultra-oligotrophic system. Fire can mobilise nutrients from soils (Kirkpatrick and Dickinson, 1984; McEachern et al., 2000; Leys et al., 2016), and initial erosive patterns following fire can increase the terrigenous material entering the lake (di Folco and Kirkpatrick, 2011; Morris et al., 2015), promoting aquatic productivity in particularly oligotrophic systems. However, the removal of organic soils and biomass caused by fire results in a long-term loss in available soils, their nutrients and subsequent reduction in aquatic productivity (Dunnette et al., 2014; Morris et al., 2015; Beck et al., 2019). This is evident in the palaeolimnological record at Lake Osborne with pulses in diatom productivity occurring at the same time as fire activity (ca. 5.8, 5.3, and 4.9 ka). These large inputs of terrigenous material and change in soil organic and nutrient content can even alter the trophic status of lakes (Beck et al., 2018b). The change in terrigenous material entering Lake Osborne influence the water clarity and lake anoxia. Lower organic content entering the lake within a *Eucalyptus* dominated catchment will decrease decomposition and increase

available oxygen and redox conditions at the bottom of lakes (Mariani et al., 2018). Fires associated with more *Eucalyptus* at Lake Osborne promoted diatoms with a preference for increased water clarity, prominent in eastern Tasmanian lakes. Additionally, during periods of frequent fires at Lake Osborne, magnetic susceptibility was high and diatom assemblages preferred higher conductivity and pH. Fire activity can increase pH and conductivity in nearby waters either: directly through mobilisation of base cations and heavy metals from bedrock and soils (Smith et al., 2011; Leys et al., 2016); through ash production- high in base cations (Korhola et al., 1996; Korsman and Segerstrom, 1998; Serieyssol et al., 2009); and inputs of burnt soils- low in organic matter with higher pH and magnetically enriched if burnt at a high temperature (400–600 °C) (Kloss et al., 2012; Haliuc et al., 2016). Thus, the consequence of increased *Eucalyptus* in a catchment causes increased erosion and changes in soil organics and promotion of fires increasing ash deposition that can alter light regimes, redox conditions, pH, conductivity, and biota in freshwater (McEachern et al., 2000; Beck et al., 2018a; Mariani et al., 2018; Beck et al., 2019).

Increases in pyrophytic vegetation during the past ca. 2.0 to 3.0 ka is a common trend across Tasmania (Fletcher et al., 2014; Beck et al., 2017; Mariani et al., 2018; Cadd et al., 2019; Mariani et al., 2019; Fletcher et al., 2020; Fletcher et al., 2021), with predictions of further increases in wildfires in Australia caused by anthropogenic climate change (Van Oldenborgh et al., 2021). In Tasmania, rainforest vegetation creates organic soils that support aquatic ecosystems through humic tannins and acid tolerant taxa. The dystrophy of many Tasmanian lakes and the number of endemic species is no coincidence as the unique ecology of Tasmanian freshwaters rely on this connection with the terrestrial environment for ideal aquatic conditions (Tyler, 1992, 1996; Walsh et al., 2004). Therefore, careful management of this environment as fire frequency and intensity increase is not only essential to protect the montane rainforest, but is also vital to protect the endemic species and aquatic environments of Tasmania – the greatest source of freshwater in Australia.

4. Conclusions

Catastrophic wildfires are becoming an increasing threat with higher temperatures and increasing drought stress brought on by climate change; however, very little is known about how fire impacts aquatic ecosystems. To better understand the impacts of fire on aquatic systems, a multiproxy palaeoecological investigation of a ca. 6.5 ka record from Lake Osborne was used to test if declines in montane rainforest drove change in the aquatic environment; if recovery of the rainforest elicit a response in the aquatic ecosystem; and how the loss of montane rainforest and shift to sclerophyll vegetation impacts the aquatic ecosystem. Our findings show fire related declines in montane rainforest from ca. 6.5 to 4.2 ka resulted in an aquatic environment that had high aquatic productivity, a diatom community indicative of higher pH and conductivity (*D. stelligera, D. tasmanica*, *F. virescens* var. *exigua*, *F. rakiuriensis, T. flocculosa, Epithemia* and *Gomphonema* spp.) due to increase erosion and ash inputs with fire activity. From ca. 4.2 to 3.0 ka, a wetter climate and low fire activity allowed montane rainforest species Cupressaceae to recover, resulting in a less productive aquatic environment and an anomalous assemblage of *Aulacoseira* diatom species with clearer waters due to less erosion and higher lake levels. A fire event at ca. 2.5 ka caused the final decline in montane rainforest taxa, replaced by Eucalypt forest. This change in vegetation resulted in increased productivity and a shift toward more eastern benthic Tasmanian diatom taxa. More sclerophyll vegetation during the past ca. 3.0 ka is widespread across Tasmania and has caused increased fire disturbance, removal of rainforest taxa and the underlying soils that support these vegetation types. Burnt soils erode into aquatic environments altering pH, productivity, light conditions, and thus species assemblages. Changes in soil organic content and vegetation in terrestrial environments caused by changing fire regimes is widespread across Tasmania. Fire related catchment changes can alter freshwater characteristics, community composition, and ecological resilience, not only in Tasmania but potentially other temperate systems globally with tightly coupled terrestrial-aquatic ecosystems. This creates an uncertain future for freshwater ecosystems sensitive to changing catchment processes.

Author contributions

K. K. Beck performed the diatom analysis, **K. M. Saunders** performed the visible reflectance spectroscopy analysis, **B. B. Wolfe** provided assistance with the interpretation of the carbon and nitrogen elemental and isotope data. Other data were provided by **M.-S. Fletcher**. Ideas for this research were conceived by **K. K. Beck, K. M. Saunders,** and **M.-S. Fletcher**. All authors contributed to the written material of the manuscript, which was led by **K. K. Beck**.

Declaration of Competing Interest

The authors declare the following financial interests/personal relationships which may be considered as potential competing interests:

Kristen Beck reports financial support was provided by University of Lincoln. Michael-Shawn Fletcher reports financial support was provided by The University of Melbourne. Brent Wolfe reports financial support was provided by Wilfrid Laurier University. Krystyna Saunders reports financial support was provided by Australian Nuclear Science and Technology Organisation. Krystyna Saunders reports financial support was provided by University of Tasmania. Michael-Shawn Fletcher reports financial support was provided by Australian Research Council. Michael-Shawn Fletcher reports financial support was provided by Fondecyt. Michael-Shawn Fletcher reports financial support was provided by US National Science Foundation.

Data availability

Following publication data will be archived with Neotoma

Acknowledgements

Thank you to the anonymous reviewers for their helpful feedback and suggestions. We would like to thank the Palawa Traditional Custodians of the land and pay respect to their Elders past and present. We extend our thanks to the Aboriginal and Torres Strait Islander people and the Tasmania National Parks and Wildlife Service. This work was funded by the Australian Research Council (ARC DIRD Project DI110100019 and ARC DP110101950), Fondecyt (3110180), and US National Science Foundation (OISE 0966472). Thank you to Scott Nichols for his help in the field and Rita Attwood for performing the charcoal analysis.

Appendix A. Supplementary data

Supplementary data to this article can be found online at https://doi.org/10.1016/j.gloplacha.2023.104077.

References

Abraham, J., Dowling, K., Florentine, S., 2017. Risk of post-fire metal mobilization into surface water resources: a review. Sci. Total Environ. 599-600, 1740–1755.
Aquatic Research Instruments, 2018. Universal Percussion Corer. Aquatic Research Instruments, Indiana, USA.
Aquino-López, M.A., 2018. Plum for ^{210}Pb chronologies. Pages Plum is an apporach to ^{210}Pb age-depth modelling that uses Bayesian statistics. https://doi.org/10.1007/s13253-13018-10328-13257.
Aquino-López, M.A., Blaauw, M., Christen, J.A., Sanderson, N.K., 2018. Bayesian Analysis of ^{210}Pb Dating. J. Agric. Biol. Environ. Stat. 23, 317–333.
Battarbee, R.W., 1986. Diatom analysis. In: Berglund, B.E. (Ed.), Handbook Palaeoecology and Palaeohydrology. John Wiley & Sons, Chichester, pp. 527–570.
Beck, K.K., Fletcher, M.-S., Gadd, P.S., Heijnis, H., Jacobsen, G.E., 2017. An early onset of ENSO influence in the extra-tropics of the Southwest Pacific inferred from a 14, 600

year high resolution multi-proxy record from Paddy's Lake, Northwest Tasmania. Quat. Sci. Rev. 157, 164–175.
Beck, K.K., Fletcher, M.S., Gadd, P.S., Heijnis, H., Saunders, K.M., Simpson, G.L., Zawadzki, A., 2018a. Variance and rate-of-change as early warning signals for a critical transition in an aquatic ecosystem state: a test case from Tasmania, Australia. J. Geophys. Res. Biogeosci. 123, 495–508.
Beck, K.K., Fletcher, M.S., Kattel, G., Barry, L.A., Gadd, P.S., Heijnis, H., Jacobsen, G., Saunders, K.M., 2018b. The indirect response of an aquatic ecosystem to long term climate-driven terrestrial vegetation in subalpine temperate Tasmania. J. Biogeogr. 45, 713–725.
Beck, K.K., Fletcher, M.S., Gadd, P., Heijnis, H., Saunders, K.M., Zawadzki, A., 2019. The long-term impacts of climate and fire on catchment processes and aquatic ecosystem response in Tasmania, Australia. Quat. Sci. Rev. 221, 105892.
Blaauw, M., Christen, J.A., 2011. Flexible paleoclimate age-depth models using an autoregressive gamma process. Bayesian Anal. 6 (3), 457–474.
Bliss, A., Prior, L.D., Bowman, D.M.J.S., 2021. Lack of reliable post-fire recovery mechanisms makes the iconic Tasmanian conifer *Athrotaxis cupressoides* susceptible to population decline. Aust. J. Bot. 69, 162–173.
Bowman, D., Jackson, W., 1981. Vegetation succession in Southwest Tasmania. Search 12, 358–362.
Bowman, D., Wood, S.W., 2009. Fire-driven land cover change in Australia and WD Jackson's theory of the fire ecology of Southwest Tasmania. In: Tropical Fire Ecology. Springer, Berlin Heidelberg, pp. 87–111.
Bowman, D., Maclean, A.R., Crowden, R.K., 1986. Vegetation-soil relations in the lowlands of south-West Tasmania. Aust. J. Ecol. 11, 141–153.
Bowman, D.M., Bliss, A., Bowman, C.J., Prior, L.D., 2019. Fire caused demographic attrition of the Tasmanian palaeoendemic conifer Athrotaxis cupressoides. Austr. Ecol. 44, 1322–1339.
Brooks, M.L., D'antonio, C.M., Richardson, D.M., Grace, J.B., Keeley, J.E., DiTomaso, J. M., Hobbs, R.J., Pellant, M., Pyke, D., 2004. Effects of invasive alien plants on fire regimes. BioScience 54, 677–688.
Brown, M.J., Crowden, R.K., Jarman, S.J., 1982. Vegetation of an alkaline pan — acidic peat mosaic in the Hardwood River Valley, Tasmania. Aust. J. Ecol. 7, 3–12.
Brugam, R.B., McKeever, K., Kolesa, L., 1998. A diatom-inferred water depth reconstruction for an Upper Peninsula, Michigan, lake. J. Paleolimnol. 20, 267–276.
Bureau of Meteorology, 2022. Climate Data Online. Page 094191 Hartz Mountain (Keoghs Pimple) TAS. Australian Goverment, Australia.
Cadd, H., Fletcher, M.S., Mariani, M., Heijnis, H., Gadd, P., 2019. The influence of fine-scale topography on the impacts of Holocene fire in a Tasmanian montane landscape. J. Quat. Sci. 34, 491–498.
Collins, L., Bradstock, R.A., Clarke, H., Clarke, M.F., Nolan, R.H., Penman, T.D., 2021. The 2019/2020 mega-fires exposed Australian ecosystems to an unprecedented extent of high-severity fire. Environ. Res. Lett. 16, 044029.
Croudace, I.W., Rothwell, R.G., 2015. Micro-XRF Studies of Sediment Cores: Applications of a Non-destructive Tool for the Environmental Sciences. Springer Science + Business Media Dordrecht, Dordrecht Heidelberg New York London.
Dean, W.E., Doner, L.A., 2012. A Holocene record of endogenic iron and manganese precipitation and vegetation history in a lake-fen complex in northwestern Minnesota. J. Paleolimnol. 47, 29–42.
Donders, T.H., Wagner-Cremer, F., Visscher, H., 2008. Integration of proxy data and model scenarios for the mid-Holocene onset of modern ENSO variability. Quat. Sci. Rev. 27, 571–579.
Dunnette, P.V., Higuera, P.E., McLauchlan, K.K., Derr, K.M., Briles, C.E., Keefe, M.H., 2014. Biogeochemical impacts of wildfires over four millennia in a Rocky Mountain subalpine watershed. New Phytol. 203, 900–912.
Faegri, K., Iversen, J., 1989. Textbook of Pollen Analysis, 4 edition. John Wiley & Sons Ltd., London, Great Britain.
Finsinger, W., Bonnici, I., 2022. Tapas: an R Package to Perform Trend and Peaks Analysis. Pages Trend and PeAkS (TAPAS) Analysis of Temporal Series (e.g. paleoecological records) to Assess Long-term Trend and Detect Events (and Eventually Estimate Event-return Intervals).
Fletcher, M.S., Bowman, D.M.J.S., Whitlock, C., Mariani, M., Beck, K.K., Stahle, L.N., Hopf, F., Benson, A., Hall, T.L., Heijnis, H., Zawadzki, A., 2021. The influence of climatic change, fire and species invasion on a Tasmanian temperate rainforest system over the past 18,000 years. Quat. Sci. Rev. 260, 106824.
Fletcher, M.-S., Wolfe, B.B., Whitlock, C., Pompeani, D.P., Heijnis, H., Haberle, S.G., Gadd, P.S., Bowman, D., 2014. The legacy of mid-Holocene fire on a Tasmanian montane landscape. J. Biogeogr. 41, 476–488.
Fletcher, M.-S., Bowman, D., Whitlock, C., Mariani, M., Stahle, L.N., 2018. The changing role of fire in conifer-dominated temperate rainforest through the last 14,000 years. Quat. Sci. Rev. 182, 37–47.
Fletcher, M.-S., Cadd, H.R., Mariani, M., Hall, T.L., Wood, S.W., 2020. The role of species composition in the emergence of alternate vegetation states in a temperate rainforest system. Landsc. Ecol. 35, 2275–2285.
di Folco, M.B., Kirkpatrick, J.B., 2013. Organic soils provide evidence of spatial variation in human-induced vegetation change following European occupation of Tasmania. J. Biogeogr. 40, 197–205.
di Folco, M.-B., Kirkpatrick, J.B., 2011. Topographic variation in burning-induced loss of carbon from organic soils in Tasmanian moorlands. Catena 87, 216–225.
Fritz, S.C., Benito, X., Steinitz-Kannan, M., 2019. Long-term and regional perspectives on recent change in lacustrine diatom communities in the tropical Andes. J. Paleolimnol. 61, 251–262.
Gallagher, R.V., Allen, S., Mackenzie, B.D., Yates, C.J., Gosper, C.R., Keith, D.A., Merow, C., White, M.D., Wenk, E., Maitner, B.S., Kang, H., Adams, V.M., Auld, T.D., 2021. High fire frequency and the impact of the 2019–2020 megafires on Australian plant diversity. Divers. Distrib. 27, 1166–1179.
Godfree, R.C., Knerr, N., Encinas-Viso, F., Albrecht, D., Bush, D., Cargill, D.C., Clements, M., Gueidan, C., Guja, L.K., Harwood, T., Joseph, L., Lepschi, B., Nargar, K., Schmidt-Lebugn, A., Broadhurst, L., 2021. Implications of the 2019–2020 megafires for the biogeography and conservation of Australian vegetation. Nat. Commun. 12, 1–13.
Gong, T., Feldstein, S.B., Luo, D., 2010. The Impact of ENSO on Wave breaking and Southern Annular Mode events. J. Atmos. Sci. 67, 2854–2870.
Haliuc, A., Hutchinson, S.M., Florescu, G., Feurdean, A., 2016. The role of fire in landscape dynamics: an example of two sediment records from the Rodna Mountains, northern Romanian Carpathians. Catena 137, 432–440.
Harris, S., Lucas, C., 2019. Understanding the variability of Australian fire weather between 1973 and 2017. PLoS One 14, e0222328.
Higuera, P., 2009. CharAnalysis 0.9: Diagnostic and Analytical Tools for Sediment Charcoal Analysis. Montana State University, Bozeman, MT.
Hill, K.J., Santoso, A., England, M.H., 2009. Interannual Tasmanian Rainfall Variability Associated with Large-Scale climate Modes. J. Clim. 22, 4383–4397.
Hill, R.S., Jordan, G.J., Macphail, M.K., 2015. Why we should retain *Nothofagus sensu lato*. Aust. Syst. Bot. 28, 190–193.
Hogg, A.G., Heaton, T.J., Hua, Q., Palmer, J.G., Turney, C.S., Southon, J., Bayliss, A., Blackwell, P.G., Boswijk, G., Ramsey, C.B., Pearson, C., Petchey, F., Reimer, P.J., Reimer, R., Wacker, L., 2020. SHCal20 Southern Hemisphere calibration, 0–55,000 years cal BP. Radiocarbon 62, 759–778.
Holz, A., Wood, S.W., Veblen, T.T., Bowman, D., 2015. Effects of high severity fire drove the population collapse of the subalpine Tasmanian endemic conifer Athrotaxis cupressoides. Glob. Chang. Biol. 21, 445–458.
Hopf, F.V.L., Colhoun, E.A., Barton, C.E., 2000. Late-glacial and Holocene record of vegetation and climate from Cynthia Bay, Lake St Clair, Tasmania. J. Quat. Sci. 15, 725–732.
IPCC, 2022. Climate Change 2022: Impacts, Adaptation, and Vulnerability. Cambridge University Press, United Kingdom.
John, J., 2018. Diatoms of Tasmania: Taxonomy and Biogeography. Koeltz Botanical Books, Kapellenbergstr.
Kilham, P., Kilham, S.S., Hecky, R.E., 1986. Hypothesized resource relationships among African planktonic diatoms. Limnol. Oceanogr. 31, 1169–1181.
Kim, B.-M., Choi, H., Kim, S.-J., Choi, W., 2017. Amplitude-dependent relationship between the Southern Annular Mode and the El Niño Southern Oscillation in austral summer. Asia-Pac. J. Atmos. Sci. 53, 85–100.
Kirkpatrick, J.B., Dickinson, K.J.M., 1984. The impact of fire on Tasmanian alpine vegetation and soils. Aust. J. Bot. 32, 613–629.
Kloss, S., Sass, O., Geitner, C., Prietzel, J., 2012. Soil properties and charcoal dynamics of burnt soils in the Tyrolean Limestone Alps. Catena 99, 75–82.
Knott, B., Suter, P.J., Richardson, A.M.M., 1978. A preliminary observation on the littoral rock Fauna of Hartz Lake and Hartz Creek, Southern Tasmania, with notes on the Water chemistry of some Neighbouring Lakes. Aust. J. Mar. Freshwat. Res. 29, 703–715.
Koinig, K.A., Shotyk, W., Lotter, A.F., Ohlendorf, C., Sturm, M., 2003. 9000 years of geochemical evolution of lithogenic major and trace elements in the sediment of an alpine lake–the role of climate, vegetation, and land-use history. J. Paleolimnol. 30, 301–320.
Korhola, A., Virkanen, J., Tikkanen, M., Blom, T., 1996. Fire-induced pH rise in a naturally acid hill-top lake, southern Finland: a palaeoecological survey. J. Ecol. 84, 257–265.
Korsman, T., Segerstrom, U., 1998. Forest fire and lake-water acidity in a northern Swedish boreal area: Holocene changes in lake-water quality at Makkassjon. J. Ecol. 86, 113–124.
Lamb, A.L., Wilson, G.P., Leng, M.J., 2006. A review of coastal palaeoclimate and relative sea-level reconstructions using $d^{13}C$ and C/N ratios in organic material. Earth Sci. Rev. 75, 29–57.
Leng, M.J., Lamb, A.L., Heaton, T.H.E., Marshall, J.D., Wolfe, B.B., Jones, M.D., Holmes, J.A., Arrowsmith, C., 2006. Isotopes in lake sediments. In: Leng, M.J. (Ed.), Isotopes in Palaeoenvironmental Research. Springer, Dordrecht, pp. 147–184.
Leys, B., Higuera, P.E., McLauchlan, K.K., Dunnette, P.V., 2016. Wildfires and geochemical change in a subalpine forest over the past six millennia. Environ. Res. Lett. 11, 125003.
Ling, H., Croome, R., Tyler, P., 1989. Freshwater dinoflagellates of Tasmania, a survey of taxonomy and distribution. Br. Phycol. J. 24, 111–129.
Macphail, M.K., 1979. Vegetation and climates in southern Tasmania since the last glaciation. Quat. Res. 11, 306–341.
Malik, H.I., Northington, R.M., Saros, J.E., 2017. Nutrient limitation status of Arctic lakes affects the responses of Cyclotella sensu lato diatom species to light: implications for distribution patterns. Polar Biol. 40, 2445–2456.
Mariani, M., Fletcher, M.S., 2016. The Southern Annular Mode determines inter-annual and centennial-scale fire activity in temperate Southwest Tasmania, Australia. Geophys. Res. Lett. 43, 1702–1709.
Mariani, M., Fletcher, M.S., 2017. Long-term climate dynamics in the southern extra-tropics revealed from sedimentary charcoal analysis. Quat. Sci. Rev. 173, 187–192.
Mariani, M., Beck, K.K., Fletcher, M.S., Gell, P., Saunders, K.M., Gadd, P., Chisari, R., 2018. Biogeochemical responses to Holocene hydroclimate fluctuations in the Tasmanian World Heritage Area, Australia. J. Geophys. Res. Biogeosci. 123, 1610–1624.
Mariani, M., Fletcher, M.-S., Haberle, S., Chin, H., Zawadzki, A., Jacobsen, G., 2019. Climate change reduces resilience to fire in subalpine rainforests. Glob. Chang. Biol. 25, 2030–2042.
Marsh, R., Mills, R.A., Green, D.R.H., Salter, I., Taylor, S., 2007. Controls on sediment geochemistry in the Crozet region. Deep-Sea Res. II Top. Stud. Oceanogr. 54, 2260–2274.

McEachern, P., Prepas, E., Gibson, J., Dinsmore, W., 2000. Forest fire induced impacts on phosphorus, nitrogen, and chlorophyll a concentrations in boreal subarctic lakes of northern Alberta. Can. J. Fish. Aquat. Sci. 57, 73–81.
McPhaden, M. J., S. E. Zebiak, and M. H. Glantz. 2006. ENSO as an Integrating Concept in Earth Science. Science 314:1740–1745.
Meyers, P.A., Teranes, J.L., 2001. Sediment Organic Matter. In: Last, W.M., Smol, J.P. (Eds.), Tracking Environmental Change Using Lake Sediments. Springer, Netherlands, pp. 239–269.
Morris, J.L., McLauchlan, K.K., Higuera, P.E., 2015. Sensitivity and complacency of sedimentary biogeochemical records to climate-mediated forest disturbances. Earth Sci. Rev. 148, 121–133.
Oksanen, J., Blanchet, F.G., Kindt, R., Legendre, P., Minchin, P.R., O'Hara, R.B., Simpson, G.L., Solymos, P., Stevens, M.H.H., Wagner, H., 2019. Package: Vegan. Pages Ordination Methods, Diversity Analysis and Other Functions for Community and Vegetation Ecologists. Community Ecology Package.
Orians, G.H., Milewski, A.V., 2007. Ecology of Australia: the effects of nutrient-poor soils and intense fires. Biol. Rev. 82, 393–423.
R Core Team, 2021. R: A Language and Environment for Statistical Computing. R Foundation for Statistical Computing, Vienna, Austria.
Rees, A.B.H., Cwynar, L.C., 2010. A test of Tyler's Line–response of chironomids to a pH gradient in Tasmania and their potential as a proxy to infer past changes in pH. Freshw. Biol. 55, 2521–2540.
Rein, B., Sirocko, F., 2002. In-situ reflectance spectroscopy – analysing techniques for high-resolution pigment logging in sediment cores. Int. J. Earth Sci. 91, 950–954.
Saros, J.E., Stone, J.R., Pederson, G.T., Slemmons, K.E.H., Spanbauer, T., Schliep, A., Cahl, D., Williamson, C.E., Engstrom, D.R., 2012. Climate-induced changes in lake ecosystem structure inferred from coupled neo- and paleoecological approaches. Ecology 93, 2155–2164.
Saros, J.E., Strock, K.E., McCue, J., Hogan, E., Anderson, J.N., 2014. Response of Cyclotella species to nutrients and incubation depth in Arctic lakes. J. Plankton Res. 36, 450–460.
Saros, J.E., Northington, R.M., Anderson, D.S., Anderson, N.J., 2016. A whole-lake experiment confirms a small centric diatom species as an indicator of changing lake thermal structure. Limnol. Oceanogr. Lett. 1, 27–35.
Saunders, K.M., Kamenik, C., Hodgson, D.A., Hunziker, S., Siffert, L., Fischer, D., Fujak, M., Gibson, J.A.E., Grosjean, M., 2012. Late Holocene changes in precipitation in Northwest Tasmania and their potential links to shifts in the Southern Hemisphere westerly winds. Glob. Planet. Chang. 92, 82–91.
Saunders, K.M., Grosjean, M., Hodgson, D.A., 2013. A 950 yr temperature reconstruction from Duckhole Lake, southern Tasmania, Australia. The Holocene 23, 771–783.
Serieyssol, C.A., Edlund, M.B., Kallemeyn, L.W., 2009. Impacts of settlement, damming, and hydromanagement in two boreal lakes: a comparative paleolimnological study. J. Paleolimnol. 42, 497–513.
Smith, H.G., Sheridan, G.J., Lane, P.N.J., Nyman, P., 2011. Wildfire effects on water quality in forest catchments: a review with implications for water supply. J. Hydrol. 396, 170–192.
Stahle, L., Whitlock, C., Haberle, S.G., 2016. A 17,000-Year-long record of vegetation and fire from Cradle Mountain National Park, Tasmania. Front. Ecol. Evol. 4, 1–17.
Stahle, L.N., Chin, H., Haberle, S., Whitlock, C., 2017. Late-glacial and Holocene records of fire and vegetation from Cradle Mountain National Park, Tasmania, Australia. Quat. Sci. Rev. 177, 57–77.
Steane, M.S., Tyler, P.A., 1982. Anomalous stratification behaviour of Lake Gorden, Headwater Reservoir of the lower Gorden River, Tasmania. Mar. Freshw. Res. 33, 739–760.
Talbot, M.R., 2001. Nitrogen Isotopes in Palaeolimnology. In: Last, W.M., Smol, J.P. (Eds.), Tracking Environmental Change Using Luke Sediments. Volume 2: Physical and Geochemical Methods. Kluwer Academic Publishers, Dordrecht, The Netherlands, pp. 401–439.
Talbot, M.R., Johannessen, T., 1992. A high resolution palaeoclimatic record for the last 27,500 years in tropical West Africa from the carbon and nitrogen isotopic composition of lacustrine organic matter. Earth Planet. Sci. Lett. 110, 23–37.
Talbot, M.R., Lærdal, T., 2000. The late Pleistocene-Holocene palaeolimnology of Lake Victoria, East Africa, based upon elemental and isotopic analyses of sedimentary organic matter. J. Paleolimnol. 23, 141–164.
Talluto, M.V., Boulangeat, I., Vissault, S., Thuiller, W., Gravel, D., 2017. Extinction debt and colonization credit delay range shifts of eastern north American trees. Nat. Ecol. Evol. 1, 1–6.
Townsend, S.A., Douglas, M.M., 2000. The effect of three fire regimes on stream water quality, water yield and export coefficients in a tropical savanna (northern Australia). J. Hydrol. 229, 118–137.
Tyler, P.A., 1992. A Lakeland from the dreamtime the second founders' lecture. Br. Phycol. J. 27, 353–368.
Tyler, P.A., 1996. 13. Endemism in freshwater algae: with special reference to the Australian region. Hydrobiologia 336, 127–135.
Van Exem, A., Debret, M., Copard, Y., Vannière, B., Sabatier, P., Marcotte, S., Laignel, B., Reyss, J.-L., Desmet, M., 2018. Hyperspectral core logging for fire reconstruction studies. J. Paleolimnol. 59, 297–308.
Van Oldenborgh, G.J., Krikken, F., Lewis, S., Leach, N.J., Lehner, F., Saunders, K.R., Van Weele, M., Haustein, K., Li, S., Wallom, D., Sparrow, S., Arrighi, J., Singh, R.K., van Aalst, M.K., Phillip, S.Y., Vautard, R., Otto, F.E.L., 2021. Attribution of the Australian bushfire risk to Anthropogenic climate change. Nat. Hazards Earth Syst. Sci. 21, 941–960.
Verschuren, D., Laird, K.R., Cumming, B.F., 2000. Rainfall and drought in equatorial East Africa during the past 1,100 years. Nature 403, 410–414.
Vyverman, W., Vyverman, R., Hodgson, D., Tyler, P., 1995. Diatoms from Tasmanian Mountain Lakes: A Reference Data-Set for Environmental Reconstruction. The TASDIAT Diatom Training Set: A Systematic and Autoecological Study. Cramer, Berlin.
Vyverman, W., Vyverman, R., Rajendran, V.S., Tyler, P., 1996. Distribution of benthic diatom assemblages in Tasmanian highland lakes and their possible use as indicators of environmental changes. Can. J. Fish. Aquat. Sci. 53, 493–508.
Walsh, R., Shiel, R., Tyler, P., 2004. Reconnaissance limnology of Tasmania VIII. Tasmanian coastal lagoons-epicentres of endemism in the Australian aquatic microbiota. In: Papers and Proceedings of the Royal Society of Tasmania, pp. 67–76.
Wolfe, A.P., Vinebrooke, R.D., Michelutti, N., Rivard, B., Das, B., 2006. Experimental calibration of lake-sediment spectral reflectance to chlorophyll a concentrations: methodology and paleolimnological validation. J. Paleolimnol. 36, 91–100.
Wolfe, B.B., Edwards, T.W.D., Aravena, R., 1999. Changes in carbon and nitrogen cycling during tree-line retreat recorded in the isotopic content of lacustrine organic matter, western Taimyr Peninsula, Russia. The Holocene 9, 215–222.
Wolfe, B.B., Edwards, T.W.D., Elgood, R.J., 2001. Carbon and Oxygen Isotope Analysis of Lake Sediment Cellulose: Methods and applications. In: Last, W.M., Smol, J.P. (Eds.), Tracking Environmental Change Using Lake Sediments. Volume 2: Physical and Geochemical Methods. Kluwer Academic Publishers, Dordrecht, The Netherlands, pp. 373–400.
Wood, S.W., Bowman, D.M.J.S., 2012. Alternative stable states and the role of fire–vegetation–soil feedbacks in the temperate wilderness of Southwest Tasmania. Landsc. Ecol. 27, 13–28.
Wood, S.W., Hua, Q., Bowman, D.M.J.S., 2011. Fire-patterned vegetation and the development of organic soils in the lowland vegetation mosaics of south-West Tasmania. Aust. J. Bot. 59, 126–136.